

Title	Data transmission at 1.3 μm using hybrid integrated silicon interposer and GaInNAs/GaAs electroabsorption modulator
Authors	Guina, Mircea;Sheehan, Robert;Isoaho, Riku;Viheriälä, Jukka;Harjanne, Mikko;Malacarne, Antonio;Falconi, Fabio;Aalto, Timo;Peters, Frank H.
Publication date	2018-11-15
Original Citation	Guina, M., Sheehan, R., Isoaho, R., ; Viheriälä, J., Harjanne, M., Malacarne, A., Falconi, F., Aalto, T. and Peters, F. H. (2018) 'Data transmission at 1.3 μm using hybrid integrated silicon interposer and GaInNAs/GaAs electroabsorption modulator', 2018 European Conference on Optical Communication (ECOC), Rome, Italy, 23 - 27 September, pp. 1-3. doi: 10.1109/ECOC.2018.8535166
Type of publication	Conference item
Link to publisher's version	10.1109/ECOC.2018.8535166
Rights	© 2018, IEEE. Personal use of this material is permitted. Permission from IEEE must be obtained for all other uses, in any current or future media, including reprinting/republishing this material for advertising or promotional purposes, creating new collective works, for resale or redistribution to servers or lists, or reuse of any copyrighted component of this work in other works.
Download date	2024-03-02 17:16:19
Item downloaded from	https://hdl.handle.net/10468/12055



UCC

University College Cork, Ireland
Coláiste na hOllscoile Corcaigh

Data Transmission at 1.3 μm Using Hybrid Integrated Silicon Interposer and GaInNAs/GaAs Electroabsorption Modulator

Mircea Guina⁽¹⁾, Robert Sheehan^(2,7), Riku Isoaho⁽¹⁾, Jukka Viheriälä⁽¹⁾, Mikko Harjanne⁽³⁾, Antonio Malacarne⁽⁴⁾, Fabio Falconi⁽⁵⁾, Timo Aalto⁽³⁾, Frank H. Peters^(6,7)

⁽¹⁾ Tampere University of Technology, 33720 Tampere, Finland, mircea.guina@tut.fi

⁽²⁾ Centre for Advanced Photonics and Process Analysis, Cork Institute of Technology, Cork, Ireland

⁽³⁾ VTT Technical Research Centre of Finland, Espoo, Finland

⁽⁴⁾ Scuola Superiore Sant'Anna, TeCIP Institute, 56124 Pisa, Italy

⁽⁵⁾ CNIT, Photonic Networks & Technologies National Laboratory, 56124 Pisa, Italy

⁽⁶⁾ Physics Department, University College Cork, Western Road, Cork, Ireland

⁽⁷⁾ Tyndall National Institute, Lee Maltings, Dyke Parade, Cork, Ireland

Abstract *Transmission of NRZ data at 12.5 Gbit/s is demonstrated using a hybrid integrated silicon photonics optical interconnect. The interconnect comprises a dilute nitride quantum well electroabsorption modulator on GaAs substrate, which is optically coupled to large core Si waveguide.*

Introduction

Demand for bandwidth intensive data and video streaming services is increasing, calling for continuous development and deployment of new optical interconnect technology in data centres¹. To this end, the use of large core Si waveguide technology, i.e. rib-waveguides², and active III–V optoelectronic devices has gained popularity for hybrid integration. The main advantages associated with using 3 μm or 12 μm thick silicon-on-insulator (SOI) waveguides are related to their insensitivity to polarization, dimensional variations, surface roughness, reduced nonlinearity, and the excellent mode match with I/O connectors and III–V active waveguides³. On the other hand, thick Si waveguides cannot be used to provide fast enough modulation in Si. Therefore, this platform requires the integration of either directly modulated lasers or electroabsorption modulators (EAMs). For example, this heterogeneous platform has been used recently to demonstrate a 400 Gbps transceiver based on the hybrid integration of directly modulated vertical-cavity surface emitting lasers and photodiode arrays operating at 1300 nm⁴. On the other hand, the deployment of active modulation with EAM has been largely limited to 1.5 μm window and InP technology.

Here we demonstrate an optical interconnect platform consisting of hybrid integrated thick Si waveguide technology and EAMs based on dilute nitride multiple quantum well (QW) materials on GaAs substrate, i.e. GaInNAs/GaAs. Dilute nitride QWs are known to provide excellent absorption properties at 1300 nm⁵, thus potentially enabling the fabrication of ultra-compact EAMs with high modulation speeds. Moreover, these materials have an advantage over InGaAsP, or AlInGaAs alloys grown on InP due to very large conduction band offset, leading

to high temperature performance⁶ with potential for un-cooled operation. These features are very important in particular for increasing the integration density and mitigating the need for active cooling at high data rates. Furthermore, the GaInNAs/GaAs platform has recently been used to demonstrate monolithic integration of 1.3 μm laser diodes on Ge substrate, opening a very promising approach for full-scale monolithic integration with Si/SiGe technology⁷. Ultimately, from the large-scale fabrication point of view, GaAs technology is compatible with microelectronics fabrication and is also benefiting from the availability of larger substrates at lower cost (i.e. 6" for GaAs compared to 4" for InP).

Modulator structure and waveguide design

The heterostructure design employed modelling of the quantum confined Stark effect (QCSE) based on acceptable parameters for dilute nitride QWs. The modulator structure incorporates 8 QWs and is shown in Tab. 1.

Tab. 1: Description of the epitaxial layer structure.

Material	Thickness (cm ⁻³)	Doping (cm ⁻³)
p-GaAs	200	10 ¹⁹
p-AlGaAs	1000	4*10 ¹⁷ – 4*10 ¹⁸
GaAs	100	
GaAsN	10	} × 8
InGaAsN	7-10	
GaAsN	10	
n-AlGaAs	1000	3*10 ¹⁷
n-GaAs	300	4*10 ¹⁷

The band structure was approximated using a 1D Poisson model⁸. Results from simulations show that the valence band offset at the GaAs-QW interface is $\Delta E_v = 0.06$ eV, while the conduction band offset is $\Delta E_c = 0.26$ eV for the chosen InGaAsN alloy. The calculated high value of conduction band offset ratio of $Q_c=0.81$ is in-

line with more advanced theoretical calculations and more importantly agrees with reported values of conduction band offset ratio for similar InGaAsN alloys⁹. Moreover, the layers are arranged in a manner that minimizes the accumulation of photo-generated holes¹⁰. The structure was grown by RF plasma-assisted molecular beam epitaxy using an established optimization routine¹¹.

The EAMs were designed to be high speed and compatible with flip-chip bonding. To accommodate both requirements, isolated pedestal high-speed contacts were used¹⁰. For these contacts, the metal was deposited on the top of the semiconductor material, where a robust metal contact can be made. Then, the large area contact was isolated from the device by etching through the epitaxial layers into the undoped semiconductor wafer. The length of the EAMs needed only be 200 μm for an extinction ratio (ER) of 10 dB. However, this was too short for cleaving and handling. As a result, additional 200 μm sections were added to the EAMs, which would be operated to transparency using a small forward bias. These sections could also be operated as low gain optical amplifiers using a larger bias. A scanning electron microscopy image of the EAM bar is shown in Fig. 1.

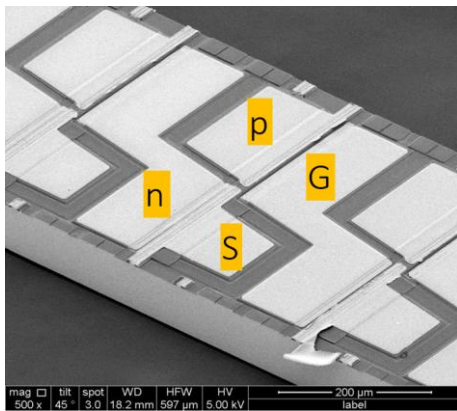


Fig. 1: Scanning electron microscope image of EAMs.

The EAM waveguide was designed to ensure alignment of its optical mode with the mode of the large core silicon waveguide after flip-chip bonding. Thus, the thickness of the EAM and the total metal thickness on the host silicon platform and on the EAM were chosen to minimise coupling losses; a schematic of alignment strategy is shown in Fig. 2. The silicon waveguide (WG) was 1.8 μm thick and was placed on top of a 3 μm oxide layer on the host silicon substrate. The cores of silicon waveguides were 6 μm wide. Thus, the EAM WG width was also increased to 6 μm to minimise mode mismatch. These wide waveguides were chosen to ease the tolerances during the passive alignment. However,

increasing the waveguide width in the EAMs resulted in a larger than intended capacitance, as described in the next section.

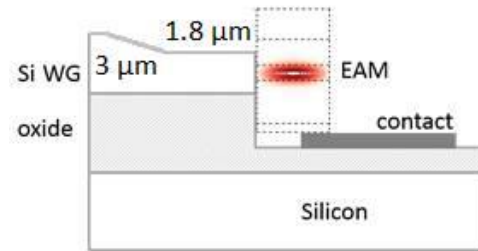


Fig. 2: Coupling between Si waveguide and EAMs.

Experimental Results

After cleaving the EAM bars, they were tested for DC and RF performance on a high-speed photonics probe station designed to accommodate bare bars. To confirm absorption based on the QCSE, the transmission through the EAM was measured as a function of input wavelength and reverse bias. The data shown in Fig. 3, reveals that the optical throughput can be substantially altered by applying a reverse bias. This is evidence for strong QCSE taking place inside the EAM. Data shows that the EAM can be operated at wavelengths around 1300 nm, where extinction ratio is 10 dB.

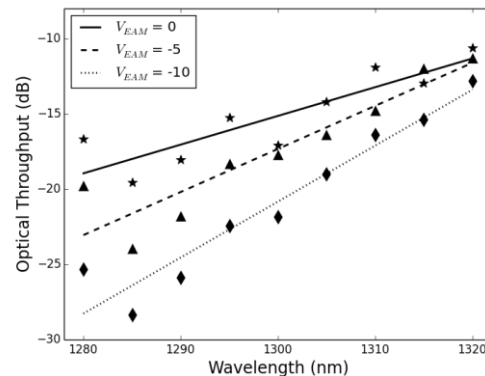


Fig. 3: Optical power transmitted through EAM under reverse bias.

The equivalent circuit of the EAMs was extracted from S_{11} reflection measurements made on the devices using a vector network analyser (VNA). The pedestal bond pads were found to have a capacitance of 38 fF, while the EAMs were found to have capacitances as high as 400 fF. A series of test bars were also characterised including EAMs with widths varying from 2 μm to 5 μm . The results shown in Fig. 4 demonstrate that the EAM capacitance can be significantly reduced by narrowing the waveguide

width, thus enabling much higher operating speeds.

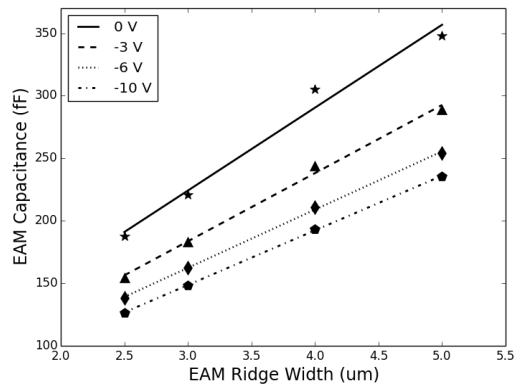


Fig. 4: EAM capacitance as a function of waveguide width for 200 μ m long EAMs.

After the EAMs were assembled on the silicon photonic modules, their large signal dynamic performance was characterised by performing a back-to-back measurement of transmitted NRZ data. Fig. 5 shows the eye diagrams from these transmission modules operating at 10 Gbps and 12.5 Gbps. At 10 Gbps the eye amplitude is 78.6 mV, and the signal to noise ratio (SNR) is 9.18 dB. At 12.5 Gbps the amplitude is 61.6 mV, and the SNR is 6.03 dB.

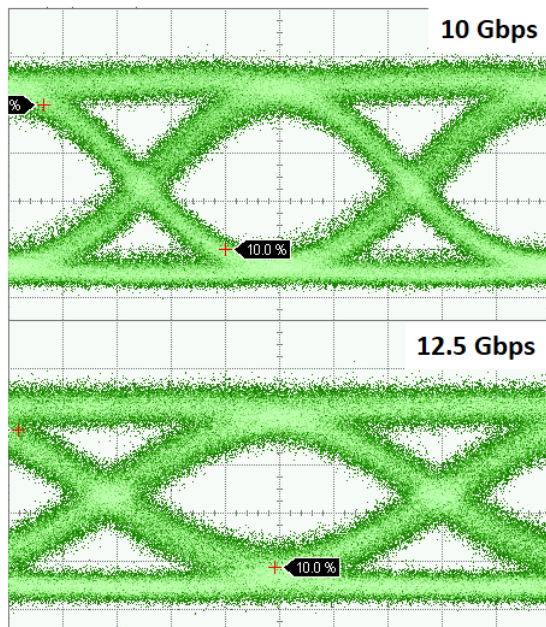


Fig. 5: 10 Gbps (top) and 12.5 Gbps (bottom) BtB eye diagrams showing operation of silicon photonics

Conclusions

Dilute nitride EAMs grown on GaAs substrates are demonstrated and integrated using passive alignment to silicon photonics transmission modules by flip-chip bonding. The devices were limited in speed due to the parasitic capacitance

of the large waveguide width EAMs but still operated at speeds up to 12.5 Gbps. The bandwidth of the devices can be scaled-up to much higher data rates by narrowing the waveguides of the EAMs. This opens the way towards a high-speed un-cooled modulation platform for hybrid integrated optical interconnects using the versatile thick SOI technology and GaAs-based dilute nitride optoelectronics platform.

Acknowledgements

Funding for the RAPIDO project, received under EU FP7-ICT-2013-11, grant agreement no.619806, is gratefully acknowledged. Arto Aho and Ville-Markus Korpiljärvi are acknowledged for support in the epitaxy.

References

- [1] C. Kachris et al., "Optical interconnection networks in data centres: Recent trends and future challenges," *IEEE Comms. Mag.*, Vol 51, no. 9 (2013).
- [2] R. A. Soref et al., "Large single-mode rib wave-guides in GeSi-Si and Si-on-SiO₂," *IEEE J. Quantum Elect.*, Vol. 27, p. 1971 (1991).
- [3] T. Aalto et al., "GaAs-SOI integration as a path to low-cost optical interconnects," *Proc. SPIE*, Vol. 7941, no. 79410S1 (2011).
- [4] T. Aalto et al., "Transceivers for 400G based on hybrid integrated thick SOI and III/V chips," in *Proc. ECOC 2017*, Gothenburg, Sweden (2017).
- [5] V. Lordi et al., "Quantum confined Stark effect in GaInNAs(Sb) quantum qells at 1300 - 1600 nm," *Appl. Phys. Lett.*, Vol. 85, no. 6 (2004)
- [6] M. Kondow et al., "GaInNAs: a novel material for long-wavelength-range laser diodes with excellent high-temperature performance", *Jpn. J. Appl. Phys.*, Vol. 35, p. 1273 (1996).
- [7] M. Guina et al., "Quantum-well laser emitting at 1.2 μ m–1.3 μ m window monolithically integrated on Ge substrate", *Proc. ECOC 2017*, paper M.1.C.3 Gothenburg, Sweden (2017).
- [8] <http://simwindows.wixsite.com/simwindows>
- [9] M. Galluppi et al., "Band offsets analysis of dilute nitride single quantum well structures employing surface photo-voltage measurements", *J. Electron. Mat.* Vol. 35, no 4, (2006).
- [10] C. L. M. Daunt et al., "Compact electroabsorption modulators for photonic integrated circuits, using an isolated pedestal contact scheme," *Photon. Technol. Lett.*, Vol. 54, no. 5, (2012).
- [11] M. Guina, S.H. Wang, book chapter "MBE of dilute nitride optoelectronic devices", in *Molecular Beam Epitaxy*, edited by M. Henini, Elsevier (2013).